

AD-A111 185

FEDERAL AVIATION ADMINISTRATION TECHNICAL CENTER ATL--ETC F/G 4/2
NUMERICAL SIMULATION OF WIND FIELDS CALCULATED FROM ASSUMED MOD--ETC(U)
JAN 82 A CARRO, R C GOFF

UNCLASSIFIED

FAA/CT-81/77

FAA-RD-81/100

NL

1 of 1
AD
A111185



END
DATE
FILMED
3 82
DTIC

14

DOT/FAA/RD-81/100
DOT/FAA/CT-81/77

Numerical Simulation of Wind Fields Calculated From Assumed Mode S Data Link Inputs

Anthony Carro
R. Craig Goff

Prepared By
FAA Technical Center
Atlantic City Airport, N.J. 08405

January 1982

Final Report

This document is available to the U.S. public
through the National Technical Information
Service, Springfield, Virginia 22161.



US Department of Transportation
Federal Aviation Administration
Systems Research & Development Service
Washington, D.C. 20590

SEARCHED
SERIALIZED
FEB 22 1982
A

AD A111185

DTIC FILE COPY

NOTICE

This document is disseminated under the sponsorship of the Department of Transportation in the interest of information exchange. The United States Government assumes no liability for the contents or use thereof.

The United States Government does not endorse products or manufacturers. Trade or manufacturer's names appear herein solely because they are considered essential to the object of this report.

1. Report No. DOT/FAA/RD-81/100	2. Government Accession No. <i>AD-A111 185</i>	3. Recipient's Catalog No.	
4. Title and Subtitle NUMERICAL SIMULATION OF WIND FIELDS CALCULATED FROM ASSUMED MODE S DATA LINK INPUTS		5. Report Date January 1982	
		6. Performing Organization Code	
7. Author(s) Anthony Carro and R. Craig Goff		8. Performing Organization Report No. DOT/FAA/CT-81/77	
		9. Performing Organization Name and Address Federal Aviation Administration Technical Center Atlantic City Airport, New Jersey 08405	
10. Work Unit No. (TRAIS)		11. Contract or Grant No. 151-412-370	
		12. Sponsoring Agency Name and Address U.S. Department of Transportation Federal Aviation Administration Systems Research and Development Service Washington, D.C. 20590	
13. Type of Report and Period Covered Final Report August 1979 - July 1981		14. Sponsoring Agency Code	
15. Supplementary Notes			
16. Abstract The future availability of the Mode S data link has suggested the possibility of using data collected by airplanes flying in the airport environment to reconstruct the atmospheric wind field in the airport area. These reconstructed fields would conceivably be of use to the metering and spacing personnel as well as to meteorologists and pilots flying through this particular atmospheric environment. An investigation was conducted to determine the feasibility of using a numerical method developed by J. T. Schaefer and C. A. Doswell III (reference 1) to produce an objectively analyzed wind field from sparse aircraft observations. A theoretical wind field resembling atmospheric conditions was used to compare the predicted field with the assumed theoretical field. Also investigated were (1) the degradation of the technique produced by decreasing the number of observations and (2) the influence of wind wavelength in the accuracy of the wind field prediction.			
17. Key Words Wind Simulation Mode S Data Link		18. Distribution Statement Document is available to the U.S. public through the National Technical Information Service, Springfield, Virginia 22161	
19. Security Classif. (of this report) Unclassified	20. Security Classif. (of this page) Unclassified	21. No. of Pages 17	22. Price

METRIC CONVERSION FACTORS

Approximate Conversions to Metric Measures

Symbol	When You Know	Multiply by	To Find	Symbol
LENGTH				
in	inches	2.5	centimeters	cm
ft	feet	30	centimeters	cm
yd	yards	0.9	meters	m
mi	miles	1.6	kilometers	km
AREA				
m ²	square inches	6.5	square centimeters	cm ²
ft ²	square feet	0.09	square meters	m ²
yd ²	square yards	0.8	square meters	m ²
mi ²	square miles	2.6	square kilometers	km ²
	acres	0.4	hectares	ha
MASS (weight)				
oz	ounces	28	grams	g
lb	pounds	0.45	kilograms	kg
	short tons	0.9	tonnes	t
	(2000 lb)			
VOLUME				
ts	teaspoons	5	milliliters	ml
Thsp	tablespoons	15	milliliters	ml
fl oz	fluid ounces	30	milliliters	ml
c	cups	0.24	liters	l
pt	pints	0.47	liters	l
qt	quarts	0.95	liters	l
gal	gallons	3.8	liters	l
ft ³	cubic feet	0.03	cubic meters	m ³
yd ³	cubic yards	0.76	cubic meters	m ³
TEMPERATURE (exact)				
°F	Fahrenheit temperature	5/9 (after subtracting 32)	Celsius temperature	°C

Approximate Conversions from Metric Measures

Symbol	When You Know	Multiply by	To Find	Symbol
LENGTH				
mm	millimeters	0.04	inches	in
cm	centimeters	0.4	inches	in
m	meters	3.3	feet	ft
km	kilometers	1.1	yards	yd
		0.6	miles	mi
AREA				
cm ²	square centimeters	0.16	square inches	in ²
m ²	square meters	1.2	square yards	yd ²
km ²	square kilometers	0.4	square miles	mi ²
ha	hectares (10,000 m ²)	2.5	acres	
MASS (weight)				
g	grams	0.035	ounces	oz
kg	kilograms	2.2	pounds	lb
t	tonnes (1000 kg)	1.1	short tons	
VOLUME				
ml	milliliters	0.03	fluid ounces	fl oz
l	liters	2.1	pints	pt
l	liters	1.06	quarts	qt
l	liters	0.26	gallons	gal
m ³	cubic meters	35	cubic feet	ft ³
m ³	cubic meters	1.3	cubic yards	yd ³
TEMPERATURE (exact)				
°C	Celsius temperature	9/5 (then add 32)	Fahrenheit temperature	°F

1 in = 2.54 centimeters exactly. 1 foot = 0.3048 meters exactly. 1 mile = 1.609344 kilometers exactly. 1 tonne = 1000 kilograms exactly. 1 short ton = 2000 pounds exactly. 1 long ton = 2240 pounds exactly. 1 liter = 1.056688 quarts exactly. 1 gallon = 4.54609 liters exactly. 1 cubic meter = 1.35348 cubic feet exactly. 1 cubic yard = 0.764555 cubic meters exactly.

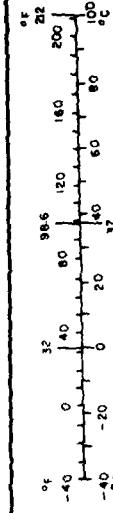


TABLE OF CONTENTS

	Page
INTRODUCTION	1
Purpose	1
Background	1
DISCUSSION	2
Brief Technique Description	2
Technical Description of the Numerical Method	2
Detailed Description of Computational Procedure	5
Numerical Simulation of Wind Fields	7
CONCLUSIONS	12
RECOMMENDATION	12
REFERENCES	14

LIST OF ILLUSTRATIONS

Figure		Page
1	Aircraft Tracks Used for Numerical Simulation	9
2	Effect of Reduction in Number of Aircraft — Simulation Grid	10
3	Increase in Data Rate	11
4	Calculated Field (No Bias and Bias)	13

INTRODUCTION

PURPOSE.

The purpose of this project was (1) to evaluate the possibility of utilizing the Schaefer-Doswell technique to objectively analyze a 3-dimensional wind field in the airport vicinity using parameters transmitted through the Mode S data link, (2) to determine the observation and aircraft density required to resolve the main features of the atmospheric wind flow in the terminal radar coverage area, and (3) to test whether this analysis could be performed in a quasi-real time frame.

BACKGROUND.

In today's air traffic control system, surveillance and communication are provided respectively by the Air Traffic Control Radar Beacon System (ATCRBS) and by very high frequency (VHF) voice radio between the pilot and the controller. The projected growth of air traffic has necessitated an increased automation of the air traffic control process. This need is being met through the development of the Mode S which combines an improved beacon interrogator/transponder system with an integral ground-air-ground data link (reference 2). This data link will make available such aircraft parameters as true airspeed and heading, which together with groundspeed and track will permit computations of the wind field in the Mode S coverage area when an adequate number of aircraft are present. The Mode S data link will supply information to a central ground-based computer which will implement one of the many available objective analysis techniques described in the meteorological literature.

The objective analysis techniques vary in complexity from simple interpolation to more advanced methods involving the solution of any number of partial differential equations. One of the techniques available is that of Schaefer-Doswell (reference 1), which combines features developed by previous investigators to try to control the growth of the errors inherent in the data collection and transmittal processes while trying to conserve the divergence and vorticity of the observations. These errors are propagated through the numerical processing used to implement the objective analysis.

Information supplied by the aircraft by means of the data link will permit the calculation of the u and v components of the wind at the aircraft locations. From these data, divergences and vorticities are calculated and, together with the u and v components of the wind vector, interpolated to the desired grid pattern. Through the numerical solution of two Poisson-type partial differential equations, an improved wind field can be produced. This method forces the wind field's divergence and vorticity to be as close to the predetermined values of the data as possible under the constraint that the winds around the boundary will correspond with those obtained by some interpolation technique. The u and v components determined can then, if desired, be converted into the magnitude and direction of the wind vector. The implementation of this numerical procedure will take approximately two minutes of processor time and 30,000 words of memory for most minicomputers.

DISCUSSION

BRIEF TECHNIQUE DESCRIPTION.

The numerical procedure used to compute an objectively analyzed wind field from known aircraft observations proceeds as follows:

1. Calculate wind components at given time intervals along the aircraft track by means of the data supplied through the Mode S data link; aircraft positions and wind components are the only information needed to implement the numerical method.
2. Select triangles with vertices at three aircraft positions by taking all aircraft positions successively, three locations at a time, to form the triangles. Equilateral triangles with smallest possible area are preferred for the calculation of the divergences and vorticities.
3. Using a Bellamy technique (reference 3), or equivalent, compute divergences and vorticities for each of the triangles selected and assign them to the triangles' centroids.
4. Interpolate wind components, divergences and vorticities to grid points using a convenient interpolation technique, such as the method described by Barnes (reference 4).
5. Solve two Poisson-type partial differential equations with Dirichlet-type boundary conditions. The values of the function on the boundary are obtained from the interpolation technique. The Poisson equations are the Euler-Lagrange equations obtained from a variational formulation (described later). The partial differential equations were solved by a finite difference procedure, which uses a second order analogue for the Laplacian operator (reference 5), the solution will produce a correction on the original interpolated wind field.

Since Mode S and its data link are not operationally available, we have introduced a known wind field to compare with the predictions of the mathematical model. This known field was obtained by using an analytical expression for the u and v components of the wind field, either directly or through the calculation of the field components from the stream function and velocity potentials, since the horizontal wind v can be partitioned into irrotational and nondivergent components

$$\underline{v} = \nabla_H \chi + k \times \nabla_H \psi \quad (1)$$

where χ is the velocity potential, ψ the stream function and ∇_H the horizontal gradient operator. The analytic expressions were selected so as to model realistic atmospheric disturbances.

TECHNICAL DESCRIPTION OF THE NUMERICAL METHOD.

The problem involves minimizing the difference between the final computed field and the interpolated field, such that the final field will have the measured divergence and vorticity. One way of doing this is to cast the problem into one of a variational type (reference 6), the functional can then be chosen as

$$J = \iint_S [(\underline{v} - \underline{\widetilde{v}})^2 + \lambda_1 (\hat{k} \cdot \nabla \times \underline{v} - \widetilde{\xi}) + \lambda_2 (\nabla \cdot \underline{v} - \widetilde{D})] dS \quad (2)$$

where:

dS is the differential surface area, $\underline{v}(x,y)$ final analyzed horizontal vector wind field, $\underline{\widetilde{v}}(x,y)$ preliminary horizontal vector wind, $\widetilde{\xi}(x,y)$ measured vertical component of vorticity, $\widetilde{D}(x,y)$ measured horizontal divergence, and λ_1, λ_2 Lagrange multipliers.

After setting the first variation equal to zero and using Green's Theorem, we get:

$$\underline{v} - \underline{\widetilde{v}} = 1/2 [\nabla \lambda_2 + \hat{k} \times \nabla \lambda_1] \quad (3)$$

$$\nabla \cdot \underline{v} = \widetilde{D} \quad (4)$$

$$\hat{k} \cdot \nabla \times \underline{v} = \widetilde{\xi} \quad (5)$$

These are the Euler-Lagrange equations. The corresponding natural boundary conditions are:

$$\oint_{\partial S} \lambda_1 \delta \underline{v} \cdot d\underline{t} = 0 \quad (6)$$

$$\oint_{\partial S} \lambda_2 \hat{k} \cdot \delta \underline{v} \times d\underline{t} = 0 \quad (7)$$

where ∂S is the boundary of the surface and \underline{t} is the tangential unit vector along the boundary curve.

From the Euler-Lagrange equations, the Lagrange multipliers satisfy the following equations:

$$\nabla^2 \lambda_1 = 2[\widetilde{\xi} - \hat{k} \cdot \nabla \times \underline{v}] \quad (8)$$

$$\nabla^2 \lambda_2 = 2[\widetilde{D} - \nabla \cdot \underline{v}] \quad (9)$$

It is necessary to solve these two partial differential equations with the above natural boundary conditions.

The simplest specification of boundary conditions that satisfy the natural boundary conditions would be:

$$\lambda_1 \Big|_{\partial S} = \lambda_2 \Big|_{\partial S} = 0 \quad (10)$$

Schaefer-Doswell (reference 1) shows that this technique gives a statistically improved wind field analysis, as compared with ordinary interpolation techniques and, at the same time, preserves the original divergence and vorticity.

This method requires the solution of two Poisson equations using numerical differentiation to find the grid-point wind components. Although the method is fairly accurate, it is computationally complicated. We will use a second method which is computationally less costly; this method produces a wind whose divergence and vorticity are as close to those measured as possible under the restriction of boundary specification of the winds.

A new variational principle is now introduced which does not include the difference $(\underline{v} - \widetilde{\underline{v}})^2$; i.e., the restriction that the difference between preliminary and analyzed field be minimal is dropped. The functional is given by:

$$I = \iint_S [(\hat{k} \cdot \nabla \times \underline{v} - \widetilde{\xi})^2 + (\nabla \cdot \underline{v} - \widetilde{D})^2] dS \quad (11)$$

After taking the first variation, this becomes:

$$m^2 \left[\frac{\partial^2}{\partial x^2} \left(\frac{u}{m} \right) + \frac{\partial^2}{\partial y^2} \left(\frac{u}{m} \right) \right] = m^2 \left[\frac{\partial}{\partial x} \left(\frac{\widetilde{D}}{m^2} \right) - \frac{\partial}{\partial y} \left(\frac{\widetilde{\xi}}{m^2} \right) \right] \quad (12)$$

$$m^2 \left[\frac{\partial^2}{\partial x^2} \left(\frac{v}{m} \right) + \frac{\partial^2}{\partial y^2} \left(\frac{v}{m} \right) \right] = m^2 \left[\frac{\partial}{\partial x} \left(\frac{\widetilde{\xi}}{m^2} \right) + \frac{\partial}{\partial y} \left(\frac{\widetilde{D}}{m^2} \right) \right] \quad (13)$$

where m is the metric coefficient determined by the analysis grid geometry.

The natural boundary conditions will be satisfied when either

$$(\nabla \cdot \underline{v} - \widetilde{D}) \Big|_{\partial S} = (\hat{k} \cdot \nabla \times \underline{v} - \widetilde{\xi}) \Big|_{\partial S} = 0 \quad (14)$$

or

$$\delta \underline{v} \Big|_{\partial S} = 0 \quad (15)$$

Because of the interrelationship between $\nabla \cdot \underline{v}$ and $\hat{k} \cdot \nabla \times \underline{v}$, the second boundary condition would be appropriate; this condition will be satisfied if the winds along the boundary are specified.

When this technique is compared with interpolation techniques, a marked improvement is shown as the domain of comparison is moved away from the boundaries (reference 7). Therefore, the quality of the wind analysis is enhanced by increasing the accuracy and number of the wind observations along the boundary. Nevertheless, when the outer grid values are omitted, a marked improvement occurs with the variational technique over the interpolation technique.

DETAILED DESCRIPTION OF COMPUTATIONAL PROCEDURE.

After computing the wind velocity components at the aircraft locations along the track, divergences and vorticities must be computed from the wind velocity components. The method described by Schaefer-Doswell will force the analyzed wind field's divergence and vorticity to be as close to the predetermined values as possible under the restriction that winds around the grid boundary will match those obtained through interpolation of the original wind observations.

The horizontal divergence D can be computed from the definition:

$$D = \nabla_H \cdot \underline{v} = \frac{\partial u}{\partial x} + \frac{\partial v}{\partial y} \quad (16)$$

This evaluation of D through the differential definition would cause two problems: (1) interpolation of winds to a uniform grid is a nonunique process and (2) a centered differences computation would underestimate the derivative. Morel and Necco (reference 8) have shown that the total uncertainty of the computation can exceed 100 percent. To avoid some of these problems (grid interpolation would no longer be necessary; discontinuities inherent in interpolation techniques would be replaced by the smoothing function of integration), the integral definition of divergence can be used:

$$D = \lim_{A \rightarrow 0} \frac{1}{A} \oint_{\partial S} \hat{k} \cdot \underline{v} \times d\underline{r} \quad (17)$$

A is the area of the surface S . We integrate around the contour of the surface, where ∂S is the curve that bounds S . Bellamy (reference 3) has developed a technique to estimate divergences using the integral definition. For the contour ∂S , we take a triangle with vertices at the wind observation locations given by the aircraft position along the aircraft's track. The winds are then allowed to displace the locations of the vertices for a small time interval δt . The divergence then equals the percentage change in area enclosed by the curve-per-unit time and is assigned to the triangle centroid. Similarly, the vertical component of vorticity ξ can be defined by:

$$\xi = \hat{k} \cdot \nabla \times \underline{v} = \frac{\partial v}{\partial x} - \frac{\partial u}{\partial y} = \lim_{A \rightarrow 0} \frac{1}{A} \oint_{\partial S} \underline{v} \cdot d\underline{r} \quad (18)$$

This can be evaluated in the same manner as the divergence, since rotating the wind vectors by 90° to the right will generate a wind field with vorticity equal to the divergence of the original field.

To construct the triangles required for the calculation of the divergences and vorticities, a circle is drawn centered around each observation sequentially. The radius is varied until between five and ten observations are included within the radius (this number is arbitrary and can be changed when convenient for the calculations). All possible combinations of three points at a time are considered, and the triangles are constructed from these three observations. The triangles with smallest area and closest to being equilateral are retained for the calculations; i.e., the triangles are weighted according to this criteria, and two more triangles than the number of observations within the circle are arbitrarily retained. After the line integrals are evaluated and a value is obtained for the divergence (or vorticity), this value is assigned to the triangle centroid. Values of the divergences and vorticities at the triangle centroids and the values of the wind components at the aircraft observation locations are then interpolated to the grid points where the wind values are desired. The grid spacing should ideally be of dimensions about half the average data spacing; however, in some situations the data and grid spacing are fixed for the particular problem and cannot be varied at will.

The next step consists of the interpolation of values to grid points in a regular array. Any of the known interpolation procedures could be used at this stage; however, we employed a technique described by Barnes (reference 4). This interpolation has a response function $D(a,k) = \exp(-a^2 k)$, where $a = 2\pi/\lambda$, λ = wavelength and k is an adjustable parameter. Barnes also considers interpolation in time with an exponential response, which we have omitted because time weighting was determined to introduce small errors when compared with other sources of error.

When the grid values are obtained, the partial differential equations

$$m^2 \left[\frac{\partial^2}{\partial x^2} \left(\frac{u}{m} \right) + \frac{\partial^2}{\partial y^2} \left(\frac{u}{m} \right) \right] = m^2 \left[\frac{\partial}{\partial x} \left(\frac{\tilde{D}}{m^2} \right) - \frac{\partial}{\partial y} \left(\frac{\tilde{\xi}}{m^2} \right) \right] \quad (19)$$

$$m^2 \left[\frac{\partial^2}{\partial x^2} \left(\frac{v}{m} \right) + \frac{\partial^2}{\partial y^2} \left(\frac{v}{m} \right) \right] = m^2 \left[\frac{\partial}{\partial x} \left(\frac{\tilde{\xi}}{m^2} \right) + \frac{\partial}{\partial y} \left(\frac{\tilde{D}}{m^2} \right) \right] \quad (20)$$

are to be solved. (m is the metric coefficient determined by the grid geometry.) As mentioned before, these equations were obtained from the variational functional:

$$I = \iint_S \{ (\hat{k} \cdot \nabla \times \underline{v} - \tilde{\xi})^2 + (\nabla \cdot \underline{v} - \tilde{D})^2 \} dS \quad (21)$$

by means of the Euler-Lagrange equations. The natural boundary conditions are now satisfied if either

$$(\nabla \cdot \underline{v} - \tilde{D})|_{\partial S} = (k \cdot \nabla \times \underline{v} - \tilde{\xi})|_{\partial S} = 0 \quad (22)$$

or

$$\delta \underline{v} |_{\partial S} = 0 \quad (23)$$

Because of the interrelationship between $\nabla \cdot \underline{v}$ and $\hat{k} \cdot \nabla \times \underline{v}$, the second condition will be used. This condition can be satisfied if the winds along the boundary are prescribed by an independent technique, such as interpolation.

To solve the partial differential equations, we have used an "Improved Second Finite Difference Analogue for the Laplacian Operator," Schaefer (reference 5). This finite difference is given by

$$\Delta F = \frac{1}{5\delta^2} \left\{ 8 [F(x+\delta, y) + F(x-\delta, y) + F(x, y+\delta) + F(x, y-\delta)] - \frac{3}{2} [F(x+\delta, y+\delta) + F(x+\delta, y-\delta) + F(x-\delta, y-\delta) + F(x-\delta, y+\delta)] - 26 F(x, y) \right\} \quad (24)$$

(δ is the grid spacing). This approximation has the property that for a general function there is a minimum of second order error and, if the function is defined only at specified points, this is the "best" possible approximation to the differential operator (acts to filter out high frequency computational wave modes in the computed Laplacian field by increasing the correlation between point-by-point values calculated by the operator and the Laplacian).

By solving these partial differential equations with the boundary conditions obtained by the interpolation scheme, an improved wind field is produced with a divergence and vorticity that will be as close as possible to the original divergence and vorticity, while the winds around the boundary will approximate those obtained by the interpolation technique.

NUMERICAL SIMULATION OF WIND FIELDS

Several numerical simulations were carried out to test the validity and accuracy of the procedure in realistic atmospheric situations. We constructed analytic wind fields, sampled them at the aircraft positions around a hypothetical airport, and these sampled wind fields were processed through the numerical scheme to be compared with the original analytic fields.

We tested analytic wind fields which consisted of one or more waves of different amplitudes, periods and orientations, and also constructed analytic wind fields from mathematical expressions for stream functions that resemble atmospheric flows (reference 9); i.e., of the form

$$\begin{aligned} \psi(x,y) = & C - Uy - Vy^2 + Wy^3 + A\sin x + B\cos 2x - E\cos x \sin y \\ & - D \left\{ 1 + \left[(x-x_0)^2 + (y-y_0)^2 \right] / L^2 \right\}^{-1/2} \end{aligned} \quad (25)$$

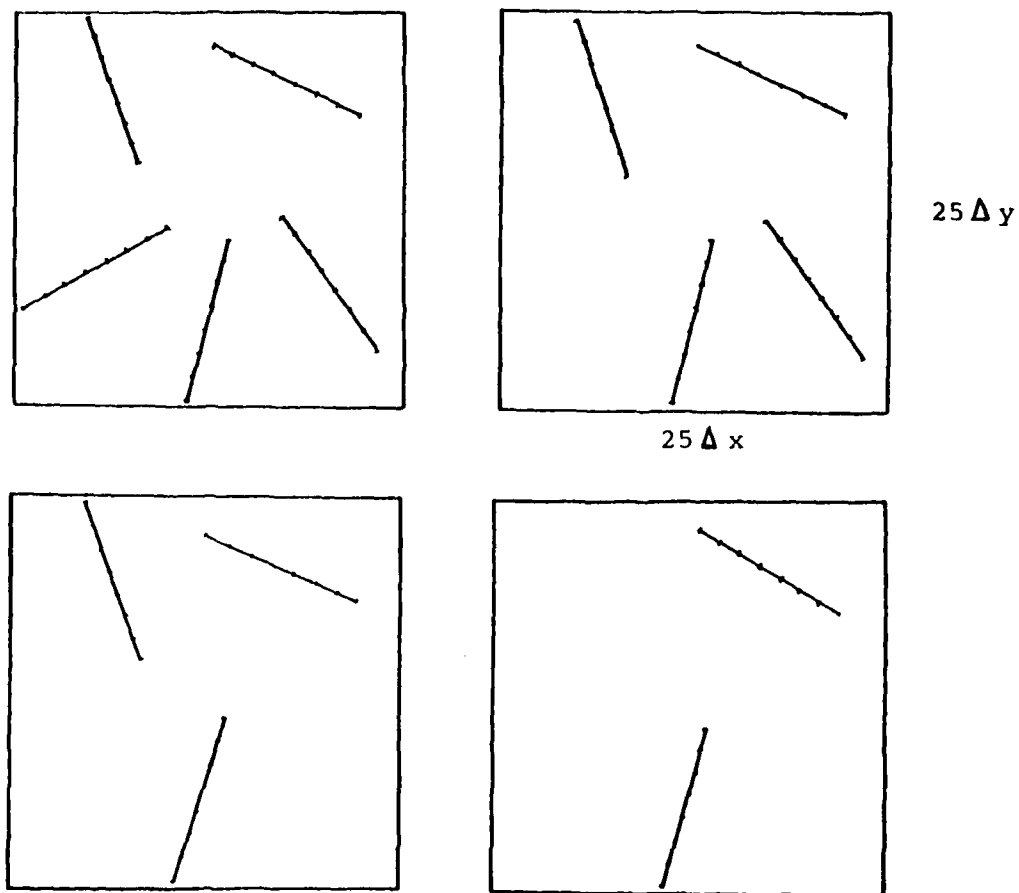
where $C, U, V, W, A, B, E, D, L, x_0$ and y_0 are constants. This was used by Schaefer and Doswell to test the divergence calculations since a field with zero divergence should be produced from a stream function.

We will comment on and show graphically the wind reconstruction for a few representative cases which will illustrate the effect of changing some of the more influential parameters; such as, the effect of reducing the number of observational aircraft within the range of the Mode S tracking antenna, the effect of changes in sample rates per aircraft, the effect of observational errors, the effect of atmospheric field wavelengths on wind field reproduction, etc.

First, we will consider a number of aircraft (the number of aircraft will be reduced from five to two) collecting data at a rate of one per 20 seconds for a period of 2 minutes and flying through an atmospheric environment (figure 1) where the u component of the wind (figure 2A) consists of a mean value of 30 units with two waves, amplitude three units and amplitude one unit respectively (units chosen are irrelevant to the numerical procedure), and period of one wave per 25 grid points (grid spacing could be considered 1 mile) (figure 2F).

The numerical method shows that, although the mean value of the field is regained by the numerical reconstructive procedure, the shape of the wave would degenerate rapidly as the number of aircraft is reduced (figure 2B to E). This rapid degeneration of the wave shape is inherent in the numerical procedure, since to calculate the divergences and vorticities, a random placement of the observations is more useful than the alignment of observations in a reduced number of aircraft tracks. The shape of the wave is no longer evident when the number of aircraft falls below three, if there is a prominent disturbance where the field has not been sampled. The improved accuracy of the field as we move away from the edges is also visible in the figure. When the number of aircraft is low, a straight interpolation procedure would be more efficient, since conservation of divergence and vorticity would not appreciably enhance the quality of the reconstruction.

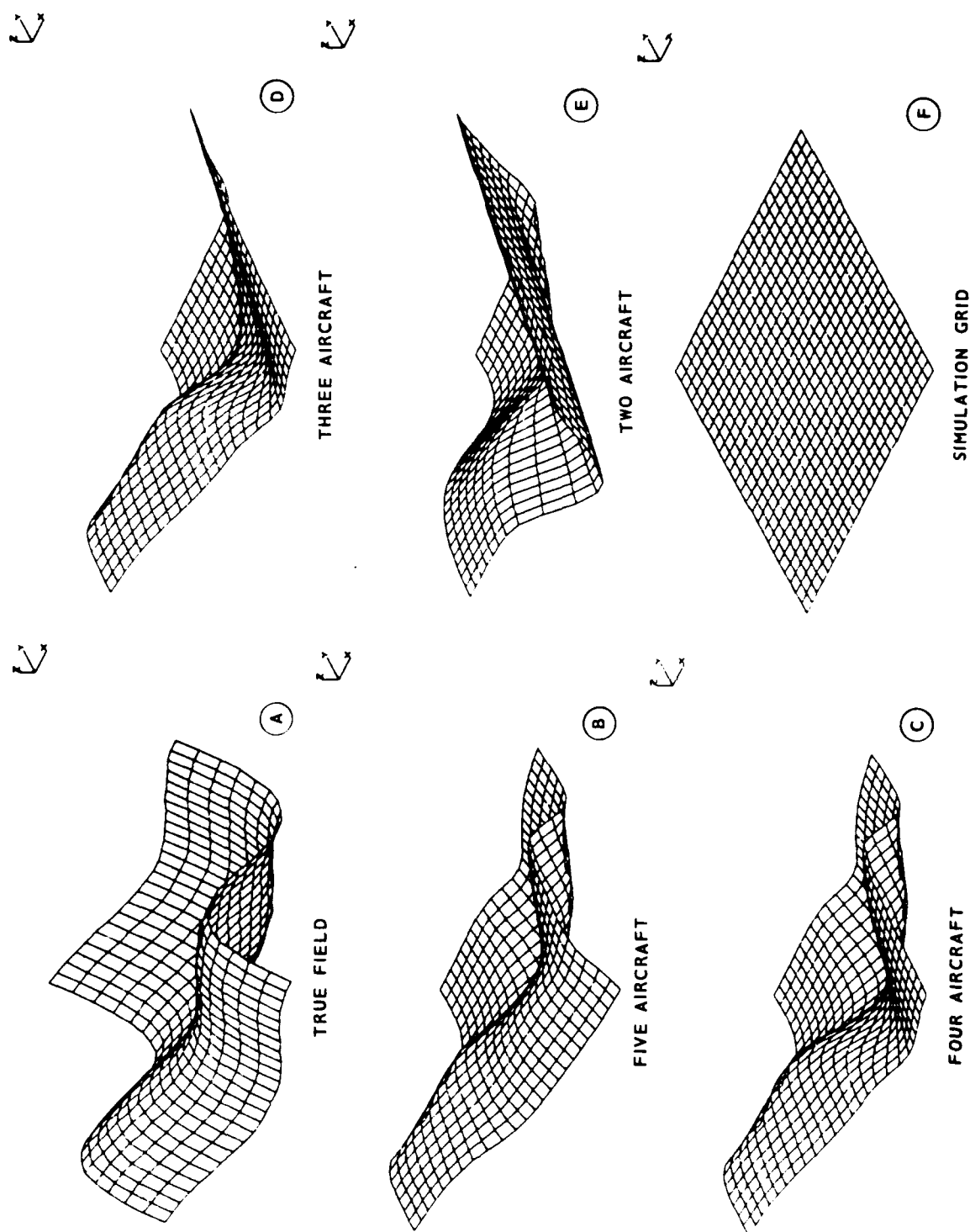
Next, we checked the effect of increasing the data rate from 20 seconds (every fifth antenna rotation) to 10 seconds and then 5 seconds, data rates that might be achieved from Mode S if required. We used the same wind field and considered the effect of the increased data rate with three aircraft collecting wind information (figure 3). As shown, the reconstruction of the field does not improve markedly, and therefore a slower sample rate of one observation every 20 seconds is sufficient. The effect of the number of aircraft is more marked than the number of observations per aircraft, even when the total number of observations is the same,



AIRCRAFT TRACKS USED FOR NUMERICAL SIMULATION

81-77-1

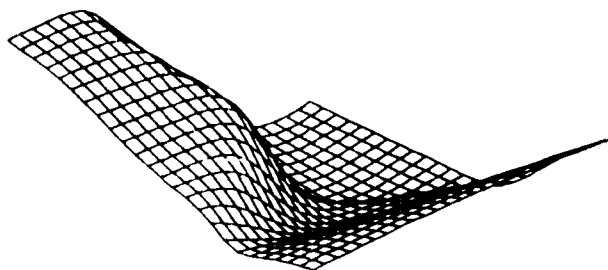
FIGURE 1. AIRCRAFT TRACKS USED FOR NUMERICAL SIMULATION



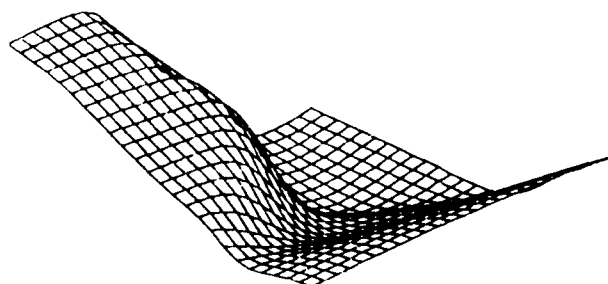
81-77-2

FIGURE 2. EFFECT OF REDUCTION IN NUMBER OF AIRCRAFT — SIMULATION GRID

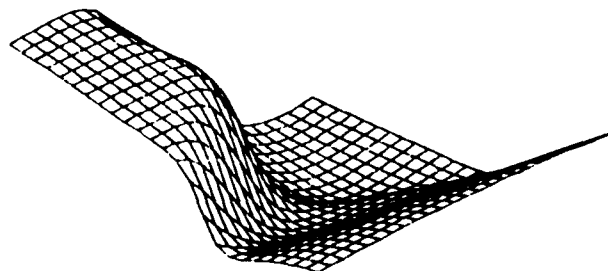
ONE OBSERVATION PER 20 SECONDS



ONE OBSERVATION PER 10 SECONDS



ONE OBSERVATION PER 5 SECONDS



81-77-3

FIGURE 3. INCREASE IN DATA RATE

since the locations of the observations are more randomly placed in this case and computations of divergence and vorticity become more reliable (there are more nearly equilateral triangles).

To show the effect of errors in the data on the numerical scheme, we introduced both a random error on all the observations and a bias on the observations from one aircraft. The random errors are reduced about a third due to the smoothing carried by the numerical method. When a bias of three units on one of five aircraft (figure 4) is introduced, we see that even in the worst possible situation when the aircraft is flying perpendicular to the wavefronts, only the field in the immediate vicinity of the biased airplane is appreciably changed. Even this bias is somewhat smoothed at the worse locations near the aircraft track.

If the number of waves per grid area is increased, the quality of the wind field reproduction deteriorates (reference 10). This is a consequence of the relationship between the mean observation separation and grid spacing. The grid spacing should be chosen to be of dimensions roughly half that of the average data spacing with the consequent limitation on the resolvable frequency of the waves.

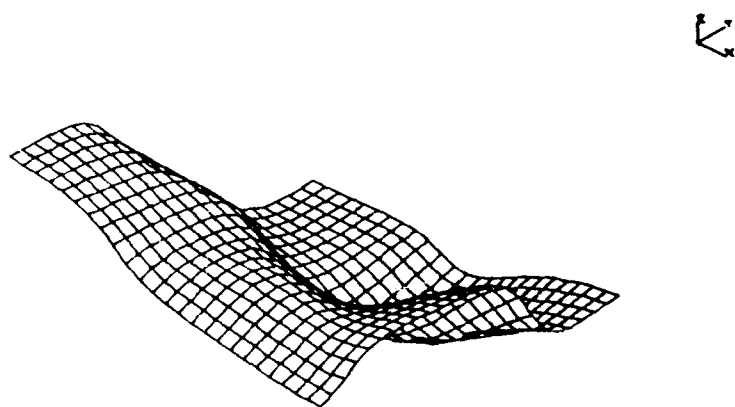
CONCLUSIONS

The Schaefer-Doswell technique was utilized to investigate wind field reconstruction from sparse observations and to simulate the effects on the numerical technique of such factors as increased data rate, changes in number of aircraft, random and biased errors, and frequency of waves. In spite of the possible degradation due to other than ideal conditions, it seems that in most circumstances this technique produces a good visualization of the atmospheric environment and an adequate numerical reconstruction of the wind field.

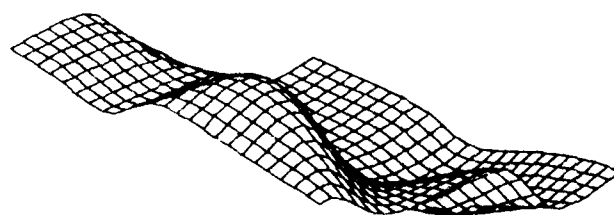
Other techniques are available which can perhaps give better results, such as the development of the first variational technique described; however, most of the techniques considered are costly in both computer time and storage, while the second variational technique used seems to be adequate for a general description of the airport wind environment.

RECOMMENDATION

While our simulation work and that of Schaefer-Doswell in the synoptic scale tend to indicate that an adequate description of the wind field is possible through this numerical technique, it would be useful to provide actual measured wind fields to the technique. As soon as the Mode S data link is available and aircraft can be equipped with Mode S transponders and wind sensors, it would be desirable to continue the technique testing. In this way, the behavior of the numerical method under actual conditions can be tested, and corrections to the numerical method or further tuning can be implemented if necessary. If more accuracy is desired, perhaps the first variational technique can be developed within our limitations of processor time and core requirements.



CALCULATED FIELD
(NO BIAS)



CALCULATED FIELD
(BIAS)

81-77-4

FIGURE 4. CALCULATED FIELD (NO BIAS AND BIAS)

REFERENCES

1. Schaefer, J.T. and Doswell III, C.A., On the Interpolation of a Vector Field. Mon. Wea. Rev., 107, 458-476, 1979.
2. Drouilhet, P.R., DABS: A System Description, Lincoln Laboratories, Lexington, Massachusetts, FAA-RD-189, 1974.
3. Bellamy, J.C., Objective Calculations of Divergence, Vertical Velocity and Vorticity. Bull. Amer. Meteor. Soc., 30, 45-49, 1949.
4. Barnes, S.L., Mesoscale Objective Map Analysis Using Weighted Time-Series Observations. NOAA Tech. Mem., NSSL-62, Normal, Oklahoma, 1973.
5. Schaefer, J.T., 1977: An Improved Second Order Finite Difference Analogue for the Laplacian Operator. J. Meteor. Soc., Japan, 55, 511-517, 1977.
6. Sasaki, Y., Some Basic Formalisms in Numerical Variational Analysis, Mon. Wea. Rev., 98-865-883, 1970.
7. Shukla, J. and Saha, K.R., Computation of Non-Divergent Stream-Function and Irrotational Velocity Potential from the Observed Winds. Mon. Wea. Rev., 102, 419-425, 1974.
8. Morel, P., and Necco, G., Scale Dependence of the 200 Sub Divergence Inferred from EOLE Data. J. Atmos. Sci., 30, 909-921, 1973.
9. Miyakoda, K., Contribution to the Numerical Weather Computation with Finite Difference, Japan J. Geophys., 3, 75-190, 1963.
10. Goff, R.C., and Carro, A., Numerical Simulation of Fields Calculated from Mode S Data link Inputs. Federal Aviation Administration Technical Center Presentation, Atlantic City, N.J., 1981.

DATE
ILME